


# Impact of Physical Topology Features on Performance of Optical Backbone Networks

Katsuaki Higashimori

NTT Network Innovation Laboratories

Kanagawa, Japan

 0000-0003-2245-8883

Takeru Inoue

NTT Network Innovation Laboratories

Takafumi Tanaka

NTT Network Innovation Laboratories

Fumikazu Inuzuka

NTT Network Innovation Laboratories

Takuya Ohara

NTT Network Innovation Laboratories

**Abstract**—Physical topology is a major determinant of the system performance of optical backbone networks, and it is important to understand the relationships between physical topology features and system performance for better system design. For application in elastic optical backbone network systems, we propose a framework of correlation analysis to examine these relationships comprehensively, and we use the framework to investigate the relationships between various physical topology features and system performance. The results of numerical experiments suggest that four important physical topology features are strongly correlated with the system performance. Specifically, the average number of hops and the *algebraic connectivity* are strongly correlated with only the communication capacity, whereas the average path length and the *geodesic distance Laplacian spectral radius* are strongly correlated with both the capacity and the cost. The *geodesic distance Laplacian spectral radius* is a newly defined quantity that is expected to expand the possibilities of physical topology design in the future. Through combinations of these features, we classify physical topology designs and examine the relationships between the classification, real networks, and graph generation algorithms.

**Keywords**—physical topology, graph feature, system performance, optical backbone network

## I. INTRODUCTION

The number of devices connected to the Internet continues to increase, and it is expected that the network capacity must continue to increase with the development of new applications [1]. Elastic optical networks (EONs) have been proposed as a means of using the frequency space more efficiently for optical backbone networks to support higher capacity. The capacity of this network system largely depends on the routing and spectrum allocation (RSA) algorithm and the physical topology. Regarding the former aspect, various algorithms have been proposed to improve the frequency utilization efficiency. The latter aspect has been shown to have an impact on the upper limit of capacity, and also to have a significant impact on EONs [2]. From a long-term perspective, the impact of the physical topology, which is difficult to install because of its cost, is particularly significant. For this reason, we focus on the physical topology in this paper.

A physical topology is generally represented as a graph, in which the nodes are communication buildings and the edges are optical fibers connecting the nodes. There are two main types of algorithms for generating such a graph: non-geometric graph models and geometric graph models. Erdos-Rényi (ER) random graph model [3] and Barabasi-Albert (BA) model, which is based on the "rich get richer" principle [4], are well-known non-geometric graph models. However, they do not include

information such as the physical distances between nodes other than the topology, and no such model has been successfully applied to describe optical backbone networks. In contrast, geometric graph models consider not only the topology but also the physical distances between nodes, and they are known to generate physical topologies that are close to those of real optical backbone networks. For example, the Waxman model is well known [5], and an improved version generates physical topologies that reproduce real networks [6]. Reference [7] compared several geometric graph models and suggested that the Gabriel graph model [8] achieves the smallest cost. Recently, the SNR-BA model, which takes into account the propagation characteristics of the optical signal in the BA model, was proposed [9]. This model rapidly generates graphs that are close to real networks and have excellent capacity and cost.

These physical topology design methods are based on accumulated knowledge of the relationship between physical topology features and system performance. For example, Baroni and Bayvel found a relationship between the topology and the number of required wavelengths [10]. Later, a relationship was found with the *algebraic connectivity* [11], a graph spectral quantity that is also closely related to the graph robustness. In addition, optimization methods that link high capacity and reliability have been proposed by using abstract graph metrics [12]. There was also an analysis on the relation between the average path length and the communication capacity [13], and from those findings, a better model was proposed [14].

Given the above background, this paper investigates the relationship between the physical topology features and system performance more comprehensively, with the aim of presenting new insights that will support future physical topology design. Our contribution is three-fold. First, we present a framework for correlation analysis to add the impact of cost to the previous findings between graph metrics and communication capacity [10, 11, 13]. Second, we classified physical topology design on the basis of the combination of key indicators extracted from the correlation analysis, and made the connection with real networks and conventional graph generation models more systematically. Third, by exploring graph features that have not been investigated in previous studies, including recent advances in spectral graph theory, we have shown a new graph feature quantity (*geodesic distance Laplacian spectral radius*) suitable for multi-objective optimization of communication capacity and cost.

The structure of this paper is as follows. In II.A, we explain the framework for correlation analysis with a higher-level view of the relationship between the physical topology and system performance. Then, II.B briefly describes the physical topology

features examined in this paper. In III.A, based on the results of the correlation analysis, we classify the features that are strongly correlated with only the communication capacity and those that are strongly correlated with both the communication capacity and the cost. We also investigate the effect of network size and extract more universally important topological features. In III.B, we classify physical topology designs on the basis of the extracted features, discuss the relationship with real networks and conventional graph generation methods, and discuss the applicability of the newly discovered metrics.

## II. SIMULATION MODEL

### A. Model for correlation analysis

Figure 1 shows an overview of the model that we use to study the relationship between physical topology features and system performance. In this paper, the optical backbone network system is assumed to have a simple model consisting of a physical topology  $G_m(V, E)$  ( $m \in \mathbb{N}$ ; the index for different physical topologies) and an RSA algorithm. The inputs to the system are the traffic matrix, which is a requirement for RSA, and the network size ( $|V|, |E|$ ) and node locations, which are requirements for the physical topology. The outputs are the communication capacity and cost. The communication capacity is considered to be the traffic load of the entire network when the request blocking rate is  $10^{-3}$ , and is defined as the traffic load tolerance  $\xi_m$ . (For practical purposes, it is desirable to define  $\xi_m$  based on a lower blocking rate. However, considering the accuracy of the evaluation of  $\xi_m$  and the computation time,  $10^{-3}$  is used as the criterion. The results for the lower blocking rate show the same trend and do not affect the discussion in this paper.)  $\text{Cost}(G_m)$  is defined in terms of total fiber length, as in previous studies of physical topologies [7]. (The cost model applied in this study is a simplified one assuming long-distance optical backbone fiber networks, and more detailed models need to be considered, especially in the case of metro networks with shorter distances [15].)

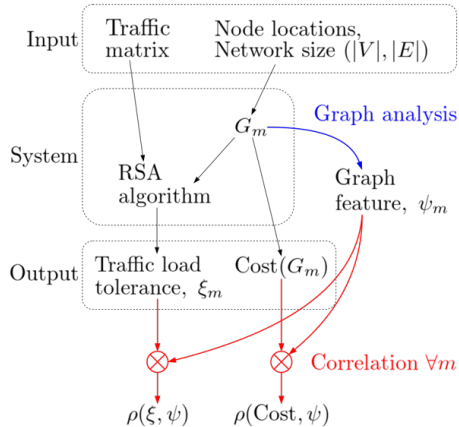


Fig. 1. Schematic view of the simulation model.

To obtain a high-level view of the relationship between physical topology features and system performance (traffic load tolerance and cost), we use an evaluation approach that includes graph analysis (right side of Figure 1) and correlation analysis (bottom of the figure). Here, the number of degrees of freedom is the number of topologies,  $n_G$ . For example, to evaluate the system response of the traffic load tolerance  $\xi = \{\xi_1, \dots, \xi_m, \dots, \xi_{n_G}\}$  to the physical topology set  $\mathcal{G} =$

$\{G_1, \dots, G_m, \dots, G_{n_G}\}$ , we calculate the following correlation coefficient:

$$\rho(\xi, \psi) = \varepsilon[(\xi - \bar{\xi})(\psi - \bar{\psi})] \cdot (\sigma_{\xi}\sigma_{\psi})^{-1}. \quad (1)$$

Here, for a variable  $x$ ,  $\varepsilon[x]$  is the expected value,  $\bar{x}$  is the ensemble mean, and  $\sigma_x$  is the standard deviation.

For RSA, we apply the routing, modulation, and spectrum allocation (RMSA) algorithm, which adaptively changes the modulation format according to the transmission distance [16]. For each candidate path calculated by the k-shortest paths method ( $k_{\max} = 8$ ), the optimal modulation format is determined for each path length, and the frequency slot size is determined according to the modulation scheme. Frequency slots are allocated by the first-fit method. The traffic matrix is assumed to be uniform, and the capacity requirement of each request is uniformly distributed within 10 -100 Gbps.

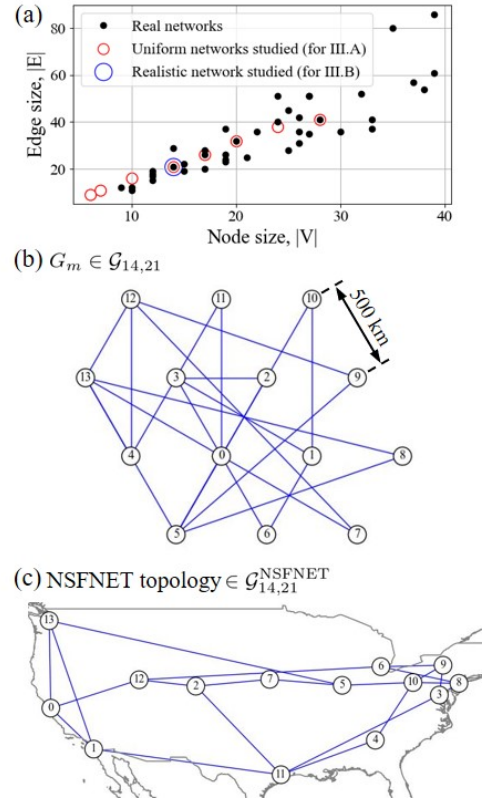


Fig. 2. (a) Distributions of real optical networks (black dots), ideal networks with uniform node locations, as studied in III.A (red circles), and a realistic network with NSFNET node locations (blue circle). The data for real optical networks are adopted from the Table 1 in [6, 9] for  $|V| < 40$ . (b) Example of a physical topology,  $G_m \in \mathcal{G}_{14,21}$ . (c) NSFNET topology.

For another system element, the physical topology, we consider a physical topology set  $\mathcal{G}_{|V|,|E|}$  that is defined for each network size, in order to examine the network size dependency in III.A. In Figure 2(a), the black dots show the distribution of real networks. In this paper, we investigate the eight network scales indicated by the red circles in the figure:  $\mathcal{G}_{6,9}$ ,  $\mathcal{G}_{7,11}$ ,  $\mathcal{G}_{10,16}$ ,  $\mathcal{G}_{14,21}$ ,  $\mathcal{G}_{17,26}$ ,  $\mathcal{G}_{20,32}$ ,  $\mathcal{G}_{24,38}$ , and  $\mathcal{G}_{28,41}$ . For each physical topology set  $\mathcal{G}_{|V|,|E|}$ , the edges of each physical topology  $G_m$  are randomly chosen from the edges of the

complete graph. Because redundancy is an essential requirement for a real network, an edge connectivity constraint of  $\kappa_E \geq 2$  is imposed on the selection process. The size  $n_G$  of each set  $\mathcal{G}_{|V|,|E|}$  (i.e., the number of topologies) is set to  $n_G = 500$ , as we found that the correlation coefficient almost converged for  $n_G \geq 400$ .

As for the node locations, we use evenly spaced locations, as shown in Figure 2(b), for the discussion in III.A. The reason for this choice is that the spatial nonuniformity of node locations differs greatly from one real network to another; accordingly, the effects of the network size and the spatial nonuniformity cannot be treated separately when comparing multiple real networks of different sizes. In a future work, we will examine the effect of the spatial nonuniformity of node locations, but in this paper, we limit the discussion to the scale dependency at spatially uniform node locations. For consistency with the discussion in III.A., III.B will show results based on a physical topology set  $\mathcal{G}_{14,21}^{NSFNET}$  that was generated from node locations similar to those of the National Science Foundation Network (NSFNET), as shown in Figure 2(c).

### B. Topological features

Physical topology features can be broadly classified into spectral and nonspectral quantities. The former are considered in terms of spectral graph theory, while the latter are widely considered in the context of complex network analysis.

First, for spectral quantities, the spectra are the eigenvalues of a graph's matrix representation, which can be the graph's Laplacian or distance Laplacian, for example. Table I lists the matrices studied in this paper. The spectra of Laplacians have been examined from various points of view, such as coloring problems and connectivity [17], while the distance Laplacian has been studied relatively recently [18]. Among the various spectral quantities, one of particular note is the second eigenvalue of the Laplacian, the *algebraic connectivity*  $a_G$ . The maximum eigenvalue of the distance Laplacian is called the *distance Laplacian spectral radius*, which has been pointed out to be related to graph coloring [19]. In this paper, we examine the maximum eigenvalue of the *geodesic distance Laplacian*, which we call the *geodesic distance Laplacian spectral radius*  $z_G$ . Through correlation analysis, we have found that it has an important relation to the optical backbone network.

TABLE I. SPECTRAL QUANTITIES

symbol	Definition
$\mathcal{L}$	Laplacian, $\mathcal{L} := \mathcal{D} - \mathcal{A}$ , where $\mathcal{A}$ and $\mathcal{D}$ respectively denote an adjacency matrix and a degree matrix.
$\mathcal{L}_g$	<i>Geodesic Laplacian</i> , i.e., the weighted Laplacian, where the weights are geodesic distances between nodes.
$\mathcal{L}^D$	Distance Laplacian, $\mathcal{L}^D := \mathcal{D}^D - \mathcal{A}^D$ . $\mathcal{A}^D$ is a distance matrix, where $\mathcal{A}_{s,d}^D$ denotes the minimum number of hops between source and destination nodes, and $\mathcal{D}^D$ is a transmission matrix.
$\mathcal{L}_g^D$	<i>Geodesic distance Laplacian</i> , $\mathcal{L}_g^D := \mathcal{D}_g^D - \mathcal{A}_g^D$ , i.e., the weighted distance Laplacian, where the weights are geodesic distances between nodes, and $\mathcal{A}_{s,d}^D$ denotes the shortest path length between source and destination nodes.

Second, the nonspectral quantities are listed in Table II. The average number of hops,  $\bar{h}$ , and the cluster coefficient  $\bar{C}$  are the most commonly used indices in complex network analysis. The global efficiency  $\bar{\eta}$  and the *geodesic global efficiency*  $\bar{\eta}_g$ , which

includes the information on physical distance, correspond to the quantities to  $\bar{h}$  and  $\bar{h}_g$ , respectively. They are used in complex network analysis as more stable features [20].

TABLE II. NONSPECTRAL QUANTITIES

symbol	Definition
$\bar{h}$	Average minimum number of hops.
$\bar{h}_g$	Average shortest path length.
$\bar{C}$	Clustering coefficient, $\bar{C} :=  V ^{-1} \sum_{v_i} [2N_i / (d_i^2 - d_i)]$ , where $N_i$ is the local triplets, and $d_i$ is the node's degree.
$\delta$	Graph diameter.
$\delta_g$	Weighted graph diameter, i.e., the maximum shortest path length.
$\bar{\eta}$	Global efficiency, $\bar{\eta} := [  V ( V  - 1) ]^{-1} \sum_{v,s,d} (\mathcal{A}_{s,d}^D)^{-1}$
$\bar{\eta}_g$	<i>Geodesic global efficiency</i> , i.e., the weighted global efficiency, defined by using the $\mathcal{A}_g^D$ of $G_m$ and that of the complete graph, $K$ : $\bar{\eta}_g := \sum_{v,s,d} [\mathcal{A}_g^D(G_m)_{s,d}]^{-1} / \sum_{v,s,d} [\mathcal{A}_g^D(K)_{s,d}]^{-1}$ .

## III. RESULTS AND DISCUSSIONS

### A. Important topology features and dependence on network size

To illustrate a typical relationship between the physical topology features and system performance, Figure 3 shows the relationship between the *algebraic connectivity*  $a_G$  and the traffic load tolerance  $\xi_m$  for  $\mathcal{G}_{14,21}$ . There is a strong correlation of 0.84 ( $\geq 0.7$ ), and the total network capacity increases in proportion to the *algebraic connectivity*. Reference [2] does not explain why the total throughput greatly depends on the physical topology, but it clearly can be explained largely by the difference in *algebraic connectivity*. The dynamic frequency assignment problem for EONs and the static wavelength assignment problem on the basis of graph coloring are dual problems; accordingly, we can see that the problem here is a rephrasing of the relationship between the number of required wavelengths and the *algebraic connectivity*, as mentioned in [11].

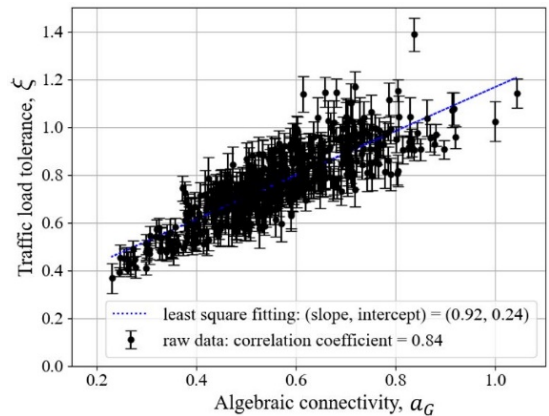


Fig. 3. Relation between *algebraic connectivity* and the traffic load tolerance for  $\mathcal{G}_{14,21}$ . The error bars were calculated from the standard deviation of the request blocking probability.

Figure 4 shows the results of the correlation analysis between the spectral quantities other than the *algebraic connectivity* and the system performance, including the cost. In the figure,  $S(\mathcal{L})$  represents the spectrum of  $\mathcal{L}$ . There are three

cases for evaluation: no correlation,  $|\rho| < 0.4$ ; correlation,  $0.4 \leq |\rho| < 0.7$ ; and strong correlation,  $0.7 \leq |\rho|$ . It can be seen that the strongest correlation with the traffic load tolerance is exhibited by the Laplacian's second eigenvalue, i.e., the *algebraic connectivity*. Moreover, among the quantities that are strongly correlated with the traffic load tolerance, the maximum value of  $S(\mathcal{L}_g^D)$ , the *geodesic distance Laplacian spectral radius*  $z_G$ , is also correlated with the cost.

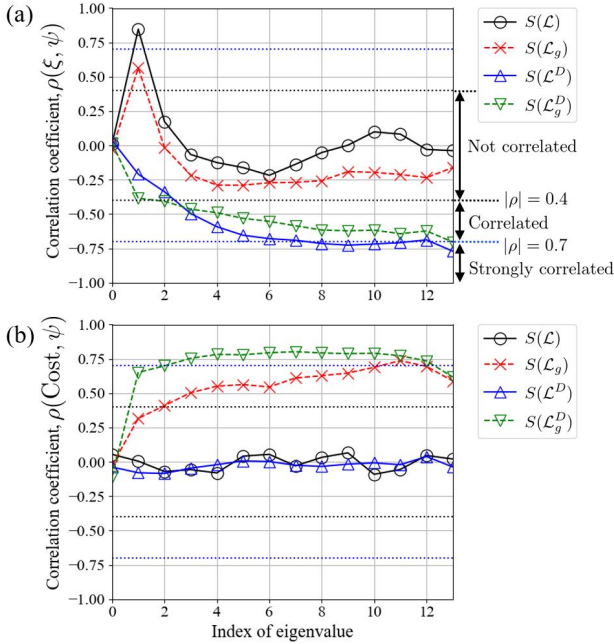


Fig. 4. Correlations between the graph's spectral quantities and the system performance indices for  $\mathcal{G}_{14,21}$ : (a)  $\rho(\xi, \psi)$  and (b)  $\rho(\text{Cost}, \psi)$ , where  $\psi = \{S(\mathcal{L}), S(\mathcal{L}_g), S(\mathcal{L}^D), S(\mathcal{L}_g^D)\}$ , and  $S(\mathcal{L})$  represents the spectrum of  $\mathcal{L}$ . The eigenvalues of these spectra  $\mu_i$  ( $i = 0, 1, \dots, |V| - 1$ ) are listed in the order  $\mu_0 \leq \mu_1 \leq \mu_2 \leq \dots \mu_{|V|-1}$ .

Figure 5 shows the results for the nonspectral quantities, along with the spectral quantities  $\{a_G, z_G\}$  extracted through the discussion for Figure 4. The quantities can be generally classified into two groups: one group is correlated only with the traffic load tolerance  $\xi$ , whereas the other group is correlated with both the traffic load tolerance and the cost. A topology focused on the communication performance can be obtained by maximizing  $\{a_G, \bar{\eta}\}$  or minimizing  $\{\delta, \bar{h}, \bar{C}\}$ . Among these quantities, the spectral quantity  $a_G$  has the strongest correlation. On the other hand, a physical topology with good traffic load tolerance and cost can be obtained by minimizing  $\{z_G, \delta_g, \bar{h}_g\}$  or maximizing  $\bar{\eta}_g$ . Among these quantities, the *geodesic distance Laplacian spectral radius*  $z_G$  has the strongest correlation with the traffic load tolerance, while  $\bar{\eta}_g$  has the strongest correlation with the cost. We exclude  $(\delta, \delta_g)$  from the following discussion because  $(\bar{h}, \bar{h}_g)$  show better correlation.

Next, Figure 6 shows the dependence of the correlation between the physical topology features and the system performance on the network size. The physical topology features  $\{a_G, \bar{h}, \bar{\eta}, \bar{C}, z_G, \bar{h}_g, \bar{\eta}_g\}$  were extracted through the discussion for Figure 5. First, we examine  $\{a_G, \bar{h}, \bar{\eta}, \bar{C}\}$ , which are correlated only with the traffic load tolerance. From Figure 6(a), the correlations for  $\{a_G, \bar{h}, \bar{\eta}\}$  become stronger as the scale increases, with  $a_G$  being the most suitable feature for optimizing

the network capacity. Because  $\bar{\eta}$  is slightly less correlated than  $\bar{h}$  and behaves in almost the same way, we exclude it from the following discussion. The cluster coefficient  $\bar{C}$  remains weakly correlated independent of the network size. Next, we examine  $\{z_G, \bar{h}_g, \bar{\eta}_g\}$ , which are correlated with both the traffic load tolerance and the cost. We exclude  $\bar{\eta}_g$  from the following discussion, because it loses its correlation with the traffic load tolerance as the network size increases. In contrast,  $\bar{h}_g$  remains correlated with both, although the correlation weakens as the network size increases.  $z_G$  behaves almost the same as  $\bar{h}_g$ : in comparison to  $\bar{h}_g$ , the cost correlation is weaker but the traffic load tolerance correlation is stronger. The choice of  $\{z_G, \bar{h}_g\}$  thus depends on whether we emphasize the communication capacity or the cost.

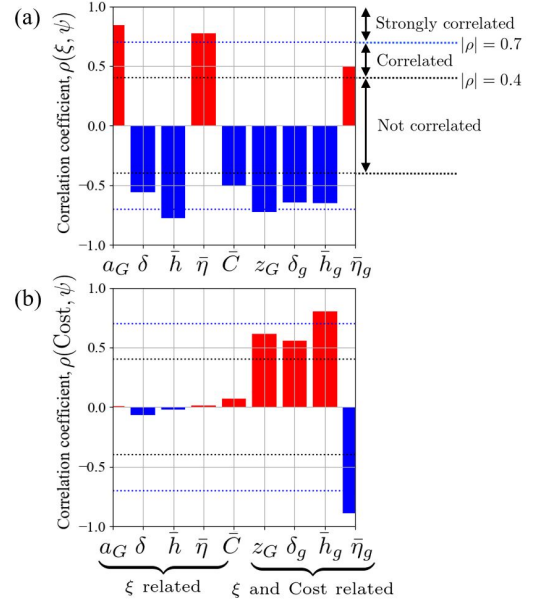


Fig. 5. Correlations between various graph quantities in  $\psi$  and system performance indices for  $\mathcal{G}_{14,21}$ : (a)  $\rho(\xi, \psi)$  and (b)  $\rho(\text{Cost}, \psi)$ .

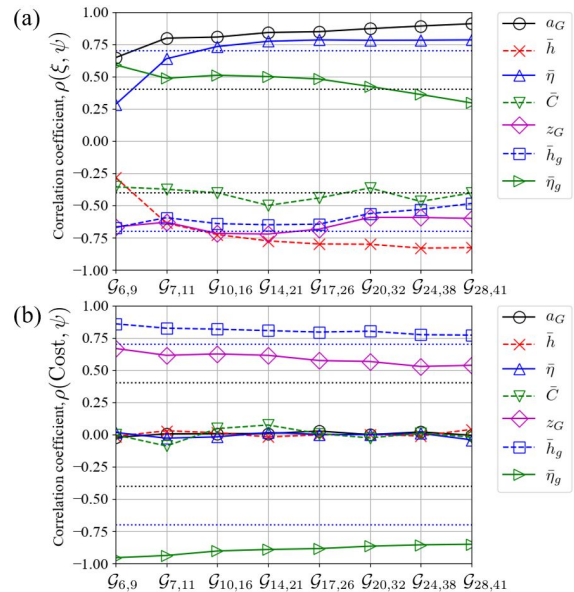


Fig. 6. Dependence of correlations, (a)  $\rho(\xi, \psi)$  and (b)  $\rho(\text{Cost}, \psi)$ , on the network size, where  $\psi = \{a_G, \bar{h}, \bar{\eta}, \bar{C}, z_G, \bar{h}_g, \bar{\eta}_g\}$ .

### B. Physical topology design classification and its relation to real networks and graph generation models

In actual physical topology design, the weights of important factors such as the communication capacity, cost, and robustness may vary depending on the system. Accordingly, it is important to understand the nature of physical topology design models and to apply an appropriate model. In this section, we examine the relationship between real networks and graph generation models and the physical topology design classification in terms of combinations of the indices extracted in III.A.

Figure 7 shows the physical topology design classification for four notable optimizations based on these combinations. The extracted indices are  $\{a_G, \bar{h}\}$ , which are strongly correlated with the traffic load tolerance;  $\{z_G, \bar{h}_g\}$ , which are strongly correlated with both the traffic load tolerance and the cost; and the cluster coefficient. By using the capacity, cost, and robustness as cutoffs, we specify the classification as (i, ii, iii, iv), which respectively correspond to optimizations that are capacity-oriented, capacity- and cost-oriented, robustness-aware capacity- and cost-oriented, and robustness-oriented. Here, robustness means that the vertex connectivity  $\kappa_V$  and the edge connectivity  $\kappa_E$  are both large. For qualitative evaluation, we also consider a column vector  $\theta = (\text{capacity}, \text{cost}, \text{robustness})^T$ . This vector is such that it gives +2 points for  $\rho \sim 0.7$  and +1 point for  $\rho \sim 0.4$ . For example, to maximize the *algebraic connectivity* on the leftmost path in the figure,  $\theta = (+2, +0, +1)^T$ . Note that the correlation between  $a_G$  and  $\bar{h}$  is as high as -0.83, as in the case of  $\mathcal{G}_{14,21}^{\text{NSFNET}}$ , and the same is true for maximizing  $-\bar{h}$ . Because the *algebraic connectivity* is related to robustness by  $a_G \leq \kappa_V \leq \kappa_E$  [21], we can say qualitatively that as the *algebraic connectivity* increases, the robustness becomes higher. Even when the *algebraic connectivity* is constant, the BA model with larger cluster coefficients becomes more robust than the ER model (e.g., as shown in Figure 8 in [22]); that is, larger cluster coefficients increase the robustness.

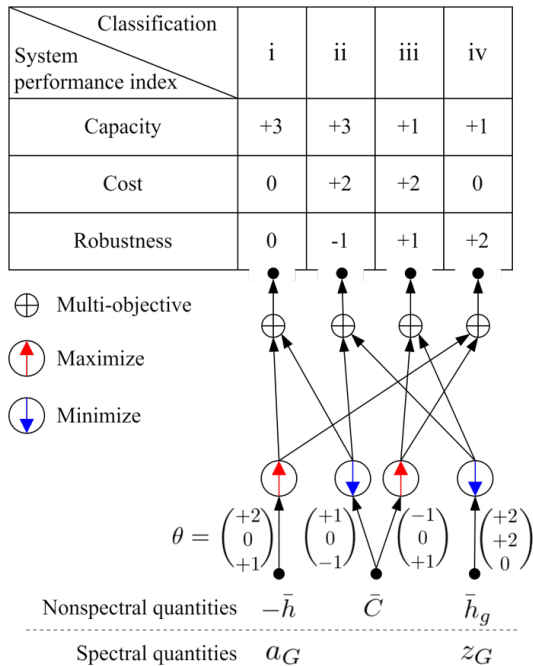


Fig. 7. Physical topology design classification diagram for optical backbone networks.

Figure 8 shows scatter plots for the physical topology set  $\mathcal{G}_{14,21}^{\text{NSFNET}}$ , with the traffic load tolerance (left) and cost (right) as color bars. The diamonds represent the average ER graph, and the stars represent the NSFNET topology. First, we use Figures 8(a) and (b) to examine the relationship between the non-geometric graph generation model and the design classification. The ER model is classified as (i) in Figure 7. The BA model generally has  $\bar{h}_{\text{BA}} \sim \bar{h}_{\text{ER}}$  and  $\bar{C}_{\text{BA}} > \bar{C}_{\text{ER}}$ , and it is classified as (iv) in Figure 7. As can be seen from Figure 8(a), the correlation between the cluster coefficient and the traffic load tolerance is weak and negative, which suggests that the communication capacity of the BA model is slightly lower than that of the ER model. In addition, Figure 8(b) clearly shows that the above graph generation method is independent of the cost.

Next, we examine the relationship with the real network, as shown in Figures 8(c) and (d). The real network was designed to have a small  $\bar{h}_g$ , and we can see that the topology is superior for EONs in terms of both the capacity and the cost. Note that this should be widely analyzed for networks besides the NSFNET, but it is at least true for networks in Germany and Europe. In addition, the cluster coefficients of real networks are widely distributed between 0 and 0.4 [6], which suggests that there is a range among categories (ii) and (iii) due to differences in design concepts.

Finally, let us consider the relation to the geometric graph generation model. The cost of the Gabriel model is small, but it has been reported that the average number of hops is large and the cluster coefficient is about 0.1-0.3 (e.g., Table 9 in [7]). With this in mind, Figure 8(a) shows that the communication capacity of the Gabriel model should be considered low, and the model is not included in categories (i-iv) described above. On the other hand, the SNR-BA model has been shown to generate topologies close to those of real optical backbone networks and to have a particularly small  $\bar{h}_g$  as compared to the ER and BA models (see Figure 10 in [9]). With this in mind, Figures 7 and 8(c) and (d) show that the SNR-BA model can be categorized as either (ii) or (iii).

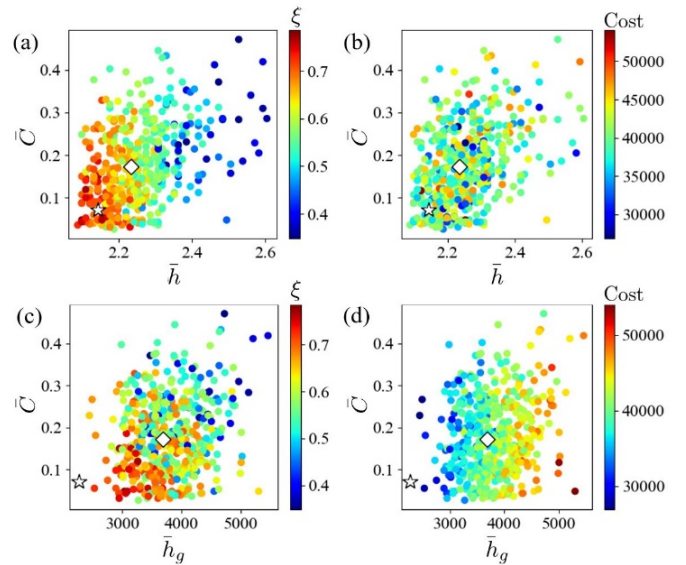


Fig. 8. Scatter plots of  $\{\bar{C}, \bar{h}\}$  and  $\{\bar{C}, \bar{h}_g\}$  for  $\mathcal{G}_{14,21}^{\text{NSFNET}}$ , with color bars indicating the traffic load tolerance  $\xi$  and the cost. The diamonds represent the average ER graph, and the stars represent the NSFNET topology.

In summary,  $\{z_G, \bar{h}_g\}$  are important indices for designing a physical topology that is close to that of a real network and has excellent communication capacity and cost. The importance of  $\bar{h}_g$  for the capacity was previously pointed out in [13], while we have investigated not only the capacity but also the cost in this paper. The newly defined *geodesic distance Laplacian spectral radius* is also important for expanding the applicability of the spectral graph theory approach. For example, for the spectral quantity of the *algebraic connectivity*, an edge addition method was proposed to generate an efficient graph [23]. We also expect that the scope of physical topology design will be expanded if it is combined with techniques such as graph sparsification [24].

#### IV. CONCLUSION

In designing a physical topology, it is important to understand the relationship between the physical topology features and system performance. In this paper, the correlation between various topology features and the system performance (communication capacity and cost) was comprehensively evaluated. From the correlation analysis results, we developed a classification of physical topology designs on the basis of combinations of highly correlated physical topology features. Moreover, we discussed the classification in terms of real networks and graph generation models. In conclusion, we have shown that the average path length and the *geodesic distance Laplacian spectral radius* are two important factors in physical topology design for optical backbone networks. In particular, the *geodesic distance Laplacian spectral radius* is a spectral quantity that has been newly defined in this paper for optical network research. We believe that it is an important finding that will enable systematical physical topology research through its connection with spectral graph theory.

We are currently working on whether the correlation between physical topology features and system performance presented in this paper holds even in the presence of nonuniformity in node locations and traffic.

#### ACKNOWLEDGMENT

Authors thank colleagues in NTT Network Innovation Laboratories for useful discussion.

#### REFERENCES

- [1] Cisco Annual Internet Report (2018–2023) White Paper [Online] (Feb. 2020), Available: <https://www.cisco.com/c/en/us/solutions/collateral/executive-perspectives/annual-internet-report/white-paper-c11-741490.html>
- [2] R. S. Tessinari, M. H. M. Paiva, M. E. Monteiro, M. E. V. Segatto, A. S. Garcia, G. T. Kanellos, R. Nejabati, and D. Simeonidou, "On the Impact of the Physical Topology on the Optical Network Performance," *IEEE British and Irish Conference on Optics and Photonics*, pp. 1–4 (2018)
- [3] P. Erdos and A. Rényi, "On the Evolution of Random Graphs", in *Publication of the Mathematical Institute of the Hungarian Academy of Sciences*, pp. 17–61 (1960)
- [4] A.-L. Barabási and R. Albert, "Emergence of scaling in random networks," *Science*, vol. 286, pp. 509–512 (1999)
- [5] B. M. Waxman, "Routing of multipoint connections," *IEEE Journal of Selected Areas in Communication*, vol. 6, no. 9, pp. 1617–1622 (1988)
- [6] C. Pavan, R. M. Morais, J. R.F. Rocha, and A. N. Pinto, "Generating Realistic Optical Transport Network Topologies," *Journal of Optical Communications and Networking*, vol. 2, no. 1, pp. 80–90 (2010)
- [7] E. K. Cetinkaya, M. J.F. Alenazi, Y. Cheng, A. M. Peck, J. P.G. Sterbenz, "A comparative analysis of geometric graph models for modelling backbone networks," *Optical Switching and Networking*, 14, pp. 95-106 (2014)
- [8] K. R. Gabriel and R. R. Sokal, "A new statistical approach to geographic variation analysis," *Syst. Zool.* 18, 259–278 (1969)
- [9] R. Matzner, D. Semrau, R. Luo, G. Zervas, and P. Bayvel, "Making intelligent topology design choices: understanding structural and physical property performance implications in optical networks," *Journal of Optical communications and Networking*, vol. 13, no. 8, pp. D53–D67 (2021)
- [10] S. Baroni and P. Bayvel, "Wavelength Requirements in Arbitrarily Connected Wavelength-Routed Optical Networks," *Journal of Lightwave Technology*, vol. 15, no. 2, pp. 242–251 (1997)
- [11] B. Châtelain, M. P. Belanger, C. Tremblay, F. Ganon, and D. V. Plant, "Topological Wavelength Usage Estimation in Transparent Wide Area Networks," *Journal of Optical Communications and Networking*, vol. 1, no. 1, pp. 196–203 (2009)
- [12] K. Higashimori, F. Inuzuka, T. Ohara, "Physical topology optimization for highly reliable and efficient wavelength-assignable optical networks," *Journal of Optical Communications and Networking*, vol. 14, no. 3, pp. 16–24 (2022)
- [13] D. Semrau, S. Durrani, G. Zervas, R. I. Killay, P. Bayvel, "On the Relationship Between Network Topology and Throughput in Mesh Optical Networks," arXiv:2008.06708v1 [cs. NI] (2020)
- [14] P. Bayvel, R. Luo, R. Matzner, D. Semrau, G. Zervas, "Intelligent design of optical networks: which topology features help maximise throughput in the nonlinear regime?" *ECOC* (2020)
- [15] K. C. Guan and V. W. S. Chan, "Cost-efficient fiber connection topology design for metropolitan area WDM networks," *Journal of Optical Communications and Networking*, vol. 1, no. 1, pp. 158-175 (2009)
- [16] L. Gong, X. Zhou, X. Liu, W. Zhao, W. Lu, Z. Zhu, "Efficient resource allocation for all-optical multicascading over spectrum-sliced elastic optical networks," *Journal of Optical Communications and Networking*, vol. 5, no. 8, pp. 836-847 (2013)
- [17] A. E. Brouwer and W. H. Haemers, "Spectra of Graphs," *Springer Press* (2011)
- [18] M. Aouchiche and P. Hansen, "Two laplacians for the distance matrix of a graph," *Linear Algebra and its Applications*, vol. 439, pp. 21–33(2013)
- [19] M. Aouchiche and P. Hansen, "Distance Laplacian eigenvalues and chromatic number in graphs," *Philomat* 31(9) pp. 2545-2555 (2017)
- [20] V. Latora, and M. Marchiori. "Efficient behavior of small-world networks." *Physical Review Letters* 87.19, pp. 198701- (2001)
- [21] M. Fiedler, "Algebraic Connectivity of Graphs," *Czechoslovak Mathematical Journal*, vol. 23, no. 2, pp. 298–305 (1973)
- [22] A. Jamakovic and S. Uhlig, "On the relationship between the algebraic connectivity and graph's robustness to node and link failures," *In Next Generation Internet Networks, Third EuroNGI Conference*, pp. 96–102 (2007)
- [23] A. Ghosh and S. Boyd, "Growing Well-connected Graphs," *Proceedings of the 45th IEEE Conference on Decision & Control*, pp. 6605–6611 (2006)
- [24] J. D. Batson, D. A. Spielman, and N. Srivastava, "Twice-Ramanujan sparsifiers," *SIAM Review*, 56(2), pp. 315-334 (2014)